Microwave and Millimeter Wave Hybrid Integrated Circuits for Radio Systems

By M. V. SCHNEIDER, BERNARD GLANCE, and W. F. BODTMANN

(Manuscript received December 16, 1968)

Hybrid integration of microwave and millimeter wave circuits is essential for achieving future communication objectives in radio systems. Hybrid integrated circuits are circuits which are manufactured on a single planar substrate. Passive elements are fabricated by partial metallization of the substrate; active devices are inserted by bonding semiconductor diodes or bulk devices to the metal conductors.

We discuss the electrical properties of passive line elements on insulating substrates. We also compare the design formulas given with measurements made at 30 GHz, and present the results obtained at 30 GHz with wideband transitions from waveguide to microstrip and the measurements obtained with microstrip IMPATT *oscillators and high order varactor multipliers in the same frequency range.*

There are advantages of scaling for building hybrid integrated circuits which we discuss. Oversize models can be built and tested in a relatively short time and substantial savings in turnaround time, required manpower, and cost can be achieved.

I. INTRODUCTION

Advances in solid-state technology and related processing techniques in recent years make it possible to produce small size, minimum weight, low production cost circuits for communication systems. These advances became possible because of simultaneous improvements in the fields of planar diffusion, photolithographic pattern delineation, and vacuum and sputtering techniques. A typical end product of this process is the beam-leaded, sealed junction monolithic integrated circuit. Although the process is extremely complex, its main advantage is that many identical circuits, untouched by human hands, can be produced in a short time at low cost.

In spite of these advances only limited progress has been achieved in applying similar concepts and techniques to circuits at microwave and millimeter wave frequencies. There are two reasons for this. One is that the planar silicon technology is not fully applicable in the microwave and millimeter wave frequency range because many types of solid-state devices are manufactured from group III-V intermetallic compounds. The other reason is that stray reactances at high frequencies are extremely important, that is, metallic overlays on semiconductors have the electrical properties of short sections of low impedance transmissiou lines which can create special circuit problems.

We show that such problems can be solved and that hybrid integrated circuits for solid-state radio systems can be built with solid-state devices mounted on or bonded to suitable metallized dielectric substrates. Circuits of this type are not complex; because they can be produced economically, they are essential in radio systems where duplicate functons are required at many repeater locations such as for the radio pole line, for high-capacity domestic satellite systems, and for *Picturephone*® see-while-you-talk-service distribution.[1,2]

The substrate, the metallization process, and the ensuing electrical properties are important factors in the design of hybrid integrated microwave circuits. We demonstrate the usefulness of scaling, which serves as an analog computer in circuit design, with data obtained from microstrip transmission line measurements, band-pass filters built at 800 MHz and 30 GHz, and measurements obtained with oversize frequency multipliers. Scaling can also be used for designing impedance transformers, microstrip circulators, and frequency converters. Excitation of hybrid modes, radiation problems, and box resonances can be easily detected and corrected in an oversize model of the final circuit. Scaling also insures substantial savings in turnaround time, required manpower, and design cost of the RF section of a repeater.

II. MICROSTRIP LINES AND SUBSTRATES

2.1 *Types of Microstrips*

Strip lines or microstrips provide the linear circuit functions in microwave integrated circuits. The lines are made by partial metallization of an insulating substrate which is supported by a metal ground plane or spaced between two ground planes with a suitable support. Two basic configurations which can be used are the standard microstrip shown in Fig. 1a and the triplate line in Fig. 1b. Both types

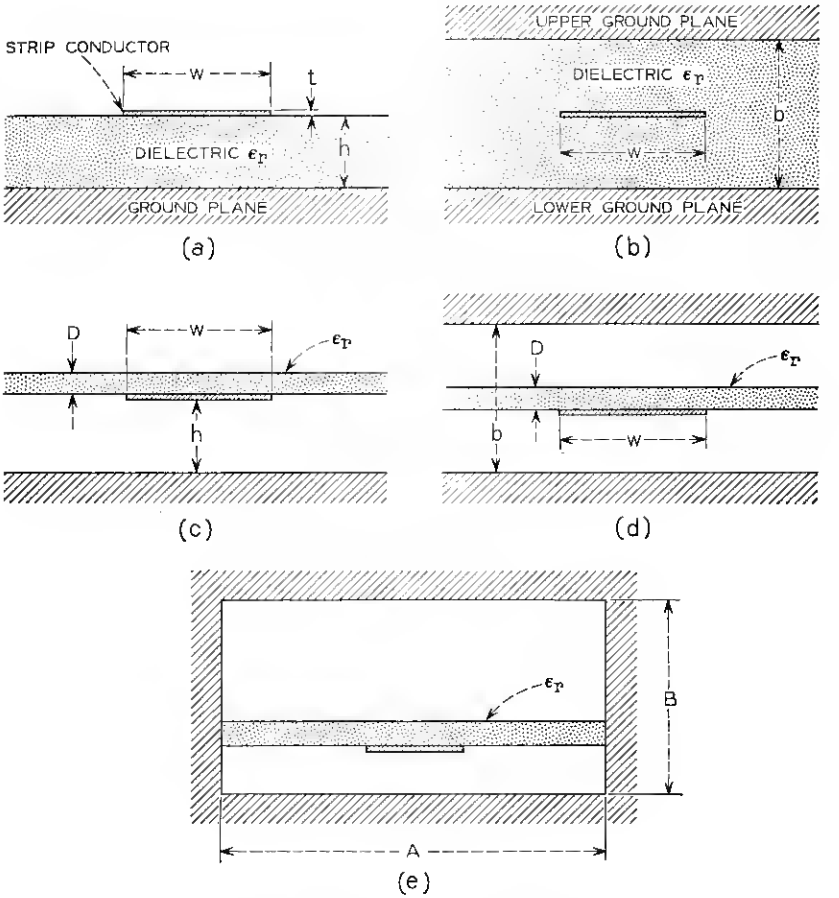

Fig. 1 — Microstrip transmission lines: (a) standard microstrip, (b) triplate microstrip embedded in dielectric, (c) inverted microstrip, (d) triplate microstrip with suspended dielectric, (e) shielded microstrip with suspended dielectric.

are used at frequencies up to a few GHz. It is often necessary to use modifications of both configurations at higher frequencies in order to obtain a low effective dielectric constant. This insures small total attenuation, improved relative mechanical tolerances, and little influence by nonuniformities of the substrate on the line parameters. The modified lines are the inverted microstrip shown in Fig. 1c and the triplate with a symmetrically suspended substrate in Fig. 1d which has been used successfully by Engelbrecht and Kurokawa for hybrid

integrated microwave transistor amplifiers.[8] The inverted microstrip and the triplate are special cases of the partially filled and completely shielded microstrip line in Fig. 1e where the major part of the field energy of a TEM mode is concentrated between one ground plane and the strip conductor, while the other ground plane and the sidewalls are used for RF shields.

2.2 *Solid-State Devices in Microstrips*

Solid-state devices in microstrips can be shunt-mounted or series-mounted. Device terminals are connected between the ground plane and the strip conductor for shunt-mounting. For series-mounting, one interrupts the strip conductor and bonds the beam-leaded device terminals to the free ends of the strip conductor. Shunt-mounts are preferred in circuits which require a good heat sink. Series-mounts are suitable if the device terminal has to be connected to a high impedance circuit. Series and shunt mounts are equivalent in most other respects with the important exception that dc biasing requirements normally determine the solution which is more economical.

Diodes and bulk devices create different circuit problems in inverted and in triplate microstrips. Radiation losses occur in standard and inverted microstrips. They can be reduced by partial or full shielding as shown in Fig. 1e. The impedance of the shielded line does not change substantially because the major part of the RF energy is still concentrated between the bottom ground plane and the strip conductor.

Another problem occurs if a solid-state device is shunt-mounted in the triplate microstrip of Fig. 1d. If the device is inserted between the lower ground plane and the strip conductor it will be shunted by the capacitance between the strip conductor and the upper ground plane. A series reactance is also added because the RF energy is about equally divided between the lower and upper half of the triplate section which does not contain a device, and is not equally divided in the section which contains the diode or the bulk device. Symmetrical distribution of the RF energy can be obtained by mounting two identical solid-state devices, one in the lower and one in the upper half of the microstrip.

2.3 *Computation of Line Parameters*

The electrical parameters of microstrips are characterized by the impedance Z, the attenuation α, the guide wavelength λ, and the unloaded Q. They can be calculated by numerical approximation as

TABLE I—MICROSTRIP IMPEDENCE

Line parameter	Standard microstrip	Triplate microstrip
Ratio $\frac{w}{h}$ or $\frac{w}{b}$	$\frac{w}{h} = \frac{2}{\pi}\frac{\partial \ln \vartheta_4(\zeta, \kappa)}{\partial \zeta}$ $\mathrm{dn}^2(2K\zeta) = E/K$	$\frac{w}{b} = -\frac{\ln k}{\pi}$ $m = k^2$
Impedance ohms	$Z_o = 60\pi\kappa$ $\kappa = K'/K$	$Z_o = \frac{60\pi}{\kappa}$ $\kappa = K'/K$
Narrow strip approximation	$w/h \ll 1$ $Z_o = 60 \ln \frac{8h}{w}$ ohm	$w/b \ll 1$ $Z_o = 60 \ln \frac{8b}{\pi w}$ ohm
Wide strip approximation	$w/h \gg 1$ $Z_o = \frac{240\pi}{2\frac{w}{h} + 5 - \frac{h}{w}}$ ohm	$w/b \gg 1$ $Z_o = \frac{30\pi}{\frac{w}{b} + \frac{\ln 4}{\pi}}$ ohm

$K(m)$, $K'(m)$, $E(m)$	Complete elliptic integrals
$m = k^2$	Modulus m
$\mathrm{dn}^2(2K\zeta) = 1 - \mathrm{sn}^2(2K\zeta)$	Jacobian elliptic function
$\vartheta_4(\zeta, \kappa)$	Theta function

shown by Brenner or by computation of Schwarz-Christoffel integrals if one assumes that the TEM mode is dominant.[4] The exact solution for the standard microstrip and the triplate microstrip of Fig. 1a and b with thickness $t = 0$ and $\epsilon_r = 1$ is given in Table I. The lines are defined by the ratios w/h or w/b which are functions of the complete elliptic integrals $K(m)$, $K'(m)$, $E(m)$ with modulus m and the logarithmic derivative of the theta function ϑ_4 defined by Tölke.[5]

The line parameters for $\epsilon_r \neq 1$ can be calculated from an effective diclectric constant ϵ_{eff} and from the line parameters for the free space microstrip Z_o, α_o, and λ_o as:

$$Z = \frac{Z_o}{(\epsilon_{eff})^{\frac{1}{2}}} \qquad \text{impedance} \qquad (1)$$

$$\lambda = \frac{\lambda_o}{(\epsilon_{eff})^{\frac{1}{2}}} \qquad \text{wavelength} \qquad (2)$$

$$\alpha = (\epsilon_{eff})^{\frac{1}{2}}\alpha_o \qquad \text{attenuation} \tag{3}$$

$$Q = Q_o = \frac{20\pi}{\ln 10}\frac{1}{\alpha_o\lambda_o} \qquad \alpha_o\lambda_o \text{ in dB.} \tag{4}$$

The free space impedance Z_o has to he computed from the equations given in Tahle I. The following approximations can he derived for the standard microstrip of Fig. 1a with $(\mu_o/\epsilon_o)^{\frac{1}{2}} = 120\pi$ ohm

$$Z_o = 60 \ln\left(\frac{8h}{w} + \frac{w}{4h}\right) \text{ ohm} \qquad \frac{w}{h} \leqq 1 \tag{5}$$

$$Z_o = \frac{120\pi \text{ ohm}}{\frac{w}{h} + 2.42 - 0.44\frac{h}{w} + \left(1 - \frac{h}{w}\right)^6} \qquad \frac{w}{h} \geqq 1. \tag{6}$$

The accuracy ohtained for strips with $w/h \leqq 10$ is ± 0.25 percent and for $w/h > 10$, the accuracy is ± 1 percent.

The effective dielectric constant ϵ_{eff} depends on the ratio w/h, the relative dielectric constant ϵ_r , and the geometrical shape of the houndary between the air and the dielectric support material. An approximation for ϵ_{eff} can he derived with an accuracy of ± 2 percent from Wheeler's theory for the standard microstrip of Fig. 1a,[6]

$$\epsilon_{eff} = \frac{\epsilon_r + 1}{2} + \frac{\epsilon_r - 1}{2}\left(1 + \frac{10h}{w}\right)^{-\frac{1}{2}}. \tag{7}$$

The conductor attenuation α_o for the standard microstrip, with the same resistivity for the ground plane and the strip conductor, can be computed from the skin resistance R_s and the partial derivatives $\partial Z_o/\partial(w/h)$ and $\partial w/\partial t$. The skin resistance is

$$R_s = (\pi\mu_o f\rho)^{\frac{1}{2}} \text{ ohm} \tag{8}$$

where f is the frequency in Hz, ρ the conductor resistivity in ohm·cm, and $\mu_o = 4\pi\cdot 10^{-9}$ H/cm. The partial derivative $\partial w/\partial t$ is obtained from an equation $Z_o = Z_o(w, h, t)$ with $Z_o =$ constant. The attenuation α_o in dB per unit length for the standard microstrip is

$$\alpha_o = -\frac{R_s}{6\pi \ln 10}\frac{\partial Z_o}{\partial\left(\frac{w}{h}\right)}\frac{1 + \frac{w}{h} + \frac{\partial w}{\partial t}}{hZ_o} \tag{9}$$

with the partial derivative $\partial w/\partial t$ given by

$$\frac{\partial w}{\partial t} = \frac{1}{\pi} \ln \frac{4\pi w}{t} \qquad \frac{w}{h} \leqq \frac{1}{2\pi} \tag{10}$$

$$\frac{\partial w}{\partial t} = \frac{1}{\pi} \ln \frac{2h}{t} \qquad \frac{w}{h} \geqq \frac{1}{2\pi}. \tag{11}$$

Equations (10) and (11) are valid for $t \ll h$, $t < w/2$, and $\partial w/\partial t > 1$. These conditions are fulfilled in most practical microstrip circuits. The attenuation obtained for narrow strips $w/h \leqq 1$ and for wide strips $w/h \geqq 1$ from equations (5), (6), and (9) in dB per unit length is

$$\alpha_c = \frac{10R_s}{\pi \ln 10} \frac{\left(\frac{8h}{w} - \frac{w}{4h}\right)\left(1 + \frac{h}{w} + \frac{h}{w}\frac{\partial w}{\partial t}\right)}{hZ_0 \exp\left(\frac{Z_0}{60}\right)} \qquad \frac{w}{h} \leqq 1 \tag{12}$$

$$\alpha_c = \frac{R_s Z_0}{720\pi^2 h \ln 10}\left[1 + \frac{0.44h^2}{w^2} + \frac{6h^2}{w^2}\left(1 - \frac{h}{w}\right)^5\right] \cdot\left(1 + \frac{w}{h} + \frac{\partial w}{\partial t}\right) \qquad \frac{w}{h} \geqq 1. \tag{13}$$

The unloaded Q can be computed from equations (4), (12), and (13).

For wide strips $w/h \gg 1$ one can compute an approximate value for α_c based on the assumption of a uniform current density in the ground plane and on the opposite bottom face of the strip conductor. By assuming that the current is uniform over the width w one obtains

$$\alpha_c = \frac{20}{\ln 10} \frac{R_s}{wZ_0} \qquad \frac{w}{h} \gg 1. \tag{14}$$

One can show that the attenuation computed from the uniform current model is always higher than the attenuation obtained from the exact theory given by equation (9). Notice that the conductor resistivity ρ at dc is always lower than the RF conductor resistivity. This explains the fact that good agreement of theory and measurement is often obtained by assuming uniform current density distribution and a skin resistance based on ρ_{dc} because the two errors tend to compensate for each other. Section 2.5 discusses a typical example.

2.4 *Dielectric Loss*

The attenuation of a microstrip is increased if the dielectric support material is lossy. If the complex dielectric constant of the substrate is

$\epsilon_r = \epsilon_r' - j\epsilon_r''$ with $\epsilon_r'' \ll \epsilon_r'$, one obtains, for the unloaded dielectric quality factor Q_D of a microstrip wbich is fully embedded in the dielectric,

$$\frac{1}{Q_D} = \tan \delta = \frac{\epsilon_r''}{\epsilon_r'}. \tag{15}$$

The line properties for partial dielectric filling are cbaracterized by an effective complex dielectric constant $\epsilon_{eff} = \epsilon_{eff}' - j\epsilon_{eff}''$. For $\epsilon_{eff}'' \ll \epsilon_{eff}'$ we obtain by partial derivation

$$\frac{\epsilon_{eff}''}{\epsilon_{eff}'} = \frac{\partial \epsilon_{eff}}{\partial \epsilon_r} \frac{\epsilon_r''}{\epsilon_{eff}'}. \tag{16}$$

Tbe unloaded quality factor for partial dielectric filling is $Q_D = \epsilon_{eff}'/\epsilon_{eff}''$ or from equations (15) and (16)

$$\frac{1}{Q_D} = (\tan \delta)_{eff} = \frac{\epsilon_r}{\epsilon_{eff}} \frac{\partial \epsilon_{eff}}{\partial \epsilon_r} \tan \delta. \tag{17}$$

Equation (17) can be simplified if the air dielectric interface is parallel to an electric field line. It is possible to define a filling factor q for sucb a line as

$$q = \frac{\partial \epsilon_{eff}}{\partial \epsilon_r} = \frac{\epsilon_{eff} - 1}{\epsilon_r - 1}. \tag{18}$$

One can show that the effective dielectric constant given by equation (7) for the standard microstrip satisfies equation (18). This can be explained by the fact that the boundary between dielectric and air is parallel to the electric field at both corners of the strip conductor where field intensities reach their maximum. For the standard microstrip one obtains from equations (17) and (18)

$$\frac{1}{Q_D} = \frac{\frac{1}{\epsilon_{eff}} - 1}{\frac{1}{\epsilon_r} - 1} \tan \delta. \tag{19}$$

The total unloaded Q of the line is

$$\frac{1}{Q_T} = \frac{1}{Q} + \frac{1}{Q_D} \tag{20}$$

with Q being the contribution from conductor loss and Q_D the contribution from dielectric loss. The attenuation α_D in dB per unit length

resulting from the dielectric is

$$\alpha_D = \frac{20\pi}{\ln 10} \frac{\frac{1}{\epsilon_{eff}} - 1}{\frac{1}{\epsilon_r} - 1} \frac{\tan \delta}{\lambda} \tag{21}$$

with λ being the guide wavelength $\lambda_0/(\epsilon_{eff})^{\frac{1}{2}}$.

2.5 *Measurements of Microstrips*

The impedance, the guide wavelength, and the effective dielectric constant of microstrips can be measured with a time domain reflectometer, a capacitance bridge, and modified slotted line techniques. The attenuation is measured with a microstrip resonator or a low loss transition from microstrip to waveguide. The measurement of line parameters is necessary because conformal mapping is often too complex and also because the skin resistance R_s is not exactly known because sufficient data for the conductor RF conductivity is lacking.

The effective dielectric constant ϵ_{eff} is an important line parameter as seen from equations (1) through (4). Computation of ϵ_{eff} is difficult for the inverted or suspended microstrip shown in Figs. 1c and d. It can be measured with a time domain reflectometer or a capacitance bridge. In the latter case, ϵ_{eff} is given by $\epsilon_{eff} = C/C_o$ with C being the capacitance with the dielectric and C_o the capacitance without the dielectric. Measurements of $(\epsilon_{eff})^{\frac{1}{2}}$ with a time domain reflectometer are shown in Fig. 2. Quartz substrates are used in the oversize microstrip transmission line. One concludes from the results of Fig. 2 that the effective dielectric constant of inverted microstrips is very low. This is also true for the shielded microstrip with suspended dielectric shown in Fig. 1e and the triplate microstrip with suspended dielectric shown in Fig. 1d.[4] The dielectric losses are small because the substrate material is located in the low field region of the microstrip.

The attenuation of a standard microstrip on a quartz substrate has been measured from 26.5 to 32 GHz with two low-loss transitions from waveguide to microstrip. The transitions are described in Section III. Line dimensions, measured and computed attenuation are given in Table II.

The calculated Q for nonuniform current distribution is based on the measured dc resistivity of the composite conductor material and a partial derivative $\partial w/\partial t = 2.1$ obtained from equation (11). A

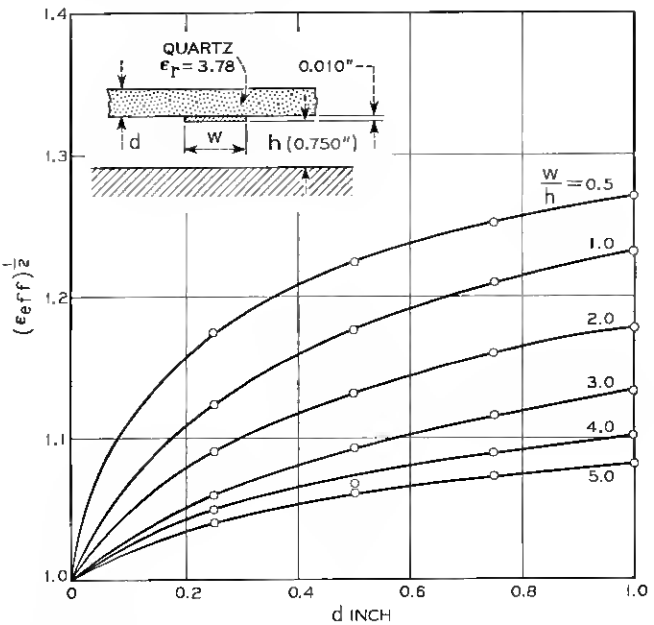

Fig. 2 — Square root of effective dielectric constant for inverted microstrip.

measurement of $\partial w/\partial t$ has been performed with an oversize microstrip line with conductor dimensions shown in Fig. 2. The partial derivative is obtained by changing the thickness t by Δt and the width w by Δw in such a way that the characteristic impedance Z_0 remains constant. Satisfactory agreement has been obtained between calculated and measured derivatives if the conductor thickness exceeds several skin depths.

2.6 *Substrate Material*

The electrical properties of the insulating substrate determine the effective dielectric constant and the dielectric losses of the microstrip. A small loss and a low ϵ_{eff} are obtained by choosing a configuration with a low RF field in the dielectric and by using a small ϵ_r. Other important design parameters are the thermal expansion coefficient and the thermal conductivity. Table III lists the properties of some substrates which can be used for microwave and millimeter wave circuits.

Clear fused and polished quartz substrates have a small surface roughness and a low ϵ_r which is independent of frequency up to a few

TABLE II—MICROSTRIP ATTENUATION AT 30 GHz

Microstrip type	Standard of Fig. 1a
Line dimensions	$w = h = 0.75$ mm, $t = 2$ μm
Clear fused polished quartz substrate*	$\epsilon_r = 3.78$
Evaporated and photoetched conductor material	150 Å nichrome (80% Ni, 20% Cr), 2 μm gold
Composite dc conductor resistivity	$\rho = 3.0 \cdot 10^{-6}$ ohm·cm
Measured attenuation 30 GHz, line length $l = 7.60$ cm	$\alpha l = 0.78$ dB
Measured unloaded Q	$Q = 450$
Calculated Q for uniform current distribution, equation (14)	$Q = 514$
Calculated Q nonuniform current distribution, equation (9)	$Q = 840$

* 99.8 per cent SiO_2, Amersil Inc., Hillside, New Jersey 07205

hundred GHz. It also has a small thermal expansion coefficient, and it is more uniform than ceramics which have to be fabricated by firing metal oxides with a suitable binder.

The least expensive material is epoxy glass which consists of a glass fiber texture with an epoxy binder. It is available as a laminate with copper cladding. Special precautions are necessary because of some moisture absorption and also because of the relatively high loss tangent.

2.7 *Metal Deposition*

Conductor materials used in microwave integrated circuits should have the following properties

TABLE III—SUBSTRATE PROPERTIES
FREQUENCY $f = 30$ GHz, ROOM TEMPERATURE $T = 25°C$

Substrate	Dielectric constant ϵ_r	Loss tangent $10^4 \cdot \tan \delta$	Thermal expansion coefficient $10^6 \cdot \alpha$ °C^{-1}	Thermal conductivity watts/cm °K
Clear fused quartz, SiO_2	3.78	1	0.4	$1.4 \cdot 10^{-2}$
Epoxy glass, Thiokol Panelite G10	4.4	80	10	$1.6 \cdot 10^{-1}$
Borosilicate glass, Corning 7040	4.5	73	4.8	$1.1 \cdot 10^{-1}$
Berillia BeO, Alsimag 754	6.0	40	6.0	2.3
Alumina Al_2O_3, Alsimag 772	9.5	1	6.0	$3.7 \cdot 10^{-1}$

(*i*) Low RF sheet resistance,
(*ii*) Good adherence and high stability,
(*iii*) Bondable top surface, and
(*iv*) Must be compatible with devices mounted into circuits.

The metal can be applied by vacuum deposition followed by electroplating. Adherence of the metal film to the substrate depends on the cleanliness of the substrate and choice of the base metal. Chromium, titanium, or nickel-chromium alloys are good base metals because of their high affinity for oxygen. A film several hundred Angstroms thick topped by an evaporated gold or copper film gives satisfactory results. The composite film must exceed several skin depths in thickness for low RF loss. The composite film should also be uniform over the total area of the circuit in order to obtain circuits which can be reproduced. Figure 3 shows a measurement of the film thickness of a nichrome-gold film over a total length of 7.5 cm. The thickness variation measured with a Tolansky-interferometer is less than ±5 percent. This result is obtained by using a three-section, three-strand tungsten coil with dimensions given in Fig. 3. The uniform film thickness leads to consistent results in the photolithographic process and in the final conductor delineation step.

III. WAVEGUIDE TO MICROSTRIP TRANSITION AT 30 GHZ

3.1 *Design of Microstrip Transitions*

The use of microstrip structures at frequencies near 30 GHz has generated a need for broadband waveguide to microstrip transitions.

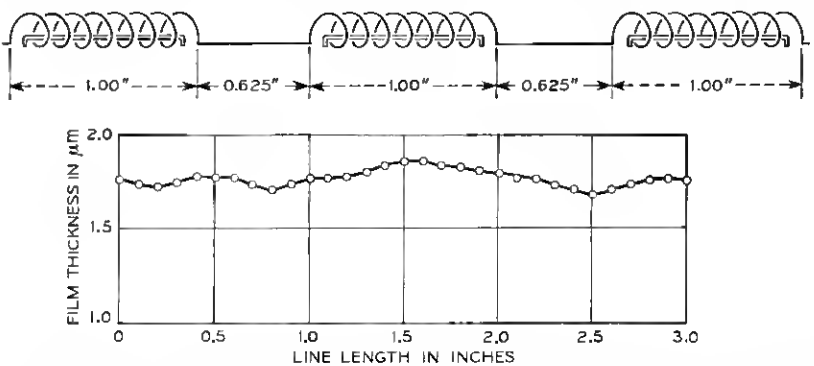

Fig. 3 — Film thickness of evaporated gold film. Tungsten coil with three sections. Gold charge: 0.060 inch diameter wire, center piece 9/16 inch long, outer pieces ¾ inch long. Distance: 2.5 inches from substrate.

Most work with microstrips has been done at frequencies below 10 GHz where coaxial-microstrip transitions have proven satisfactory;[7,8] however, at higher frequencies test equipment is usually supplied with waveguide connectors, and waveguide-to-microstrip transistions are needed to determine the performance of microstrip components. The desirable features of such a transition are that it:

(*i*) Has a high return loss so that it does not appreciably effect loss or reflection measurements made on microstrip components.

(*ii*) Has a low transmission loss.

(*iii*) Can be connected to the microstrip with reproducable results and is easily connected or removed.

(*iv*) Be an in-line design for ease of connecting to test equipment.

(*v*) Is mechanically easy to reproduce.

The design approach has been to transform from the waveguide impedance to the microstrip impedance by use of a broadband stepped ridgeline transformer which is mechanically connected to the microstrip by a tab and a single pressure screw. The reactance introduced at the ridgeline-microstrip junction can be made sufficiently small so that the final transition satisfies the five desirable features just listed.

3.2 *Transformer*

A broadband four-step transformer is used to match the impedance of the RG-96/U waveguide to that of the microstrip. For a given bandwidth and return loss, the desired impedance at each step is computed by the design method outlined in Ref. 9. A stepped single ridgeline was chosen for this transformer since it is readily adapted to the unsymmetrical microstrip line; this type of structure is easily machined and attached to the waveguide. The mechanical dimensions of a ridgeline required to achieve the desired impedance at each step can be computed from the extensive data on ridgeline given in Ref. 10. By setting the height of the last step so that the substrate will hit and stop against the ridgeline, the microstrip ridgeline junction is made in a reproducible way. For a given waveguide size and impedance, choosing the height of the ridgeline also determines the width.[10] The ridgeline used in this transition is 0.096 inch wide.

3.3 *Performance of Transition*

The frequency band of interest is the band between 27.5 and 31.3 GHz. The return loss of a four-step ridgeline transformer designed for

this band, as shown in Fig. 4, curve 1, is substantially greater than 30 dB. The return loss of the complete transition is shown by curve 2 of Fig. 4. The reactance at the microstrip-ridgeline junction has been decreased by tapering the edge of the transformer at the junction. As curve 2 shows, the junction reactance decreased the return loss over the center of the band, improved the performance of the transformer at higher frequencies, and extended the useful bandwidth of the transition. This transition has more than 30 dB return loss over a 17 percent bandwidth and an insertion loss less than 0.1 dB.

3.4 *Mechanical Design*

The mechanical arrangement is shown by Fig. 5a. The waveguide and substrate are clamped to a common base for rigidity; a single insulated pressure screw (not shown) connects the 0.020-inch tab to the 0.030-inch-wide microstrip and applies pressure to the microstrip-waveguide ground planes. The edge of the ridgeline is used as a stop to position the substrate. This transition can be readily connected or removed without damaging the microstrip ground plane or line. Figure 5b shows the dimensions of the ridgeline transformer.

3.5 *Microstrip Line*

The microstrip conductor is deposited by evaporating a 2 μm thick gold film on a 0.030-inch clear fused and polished quartz substrate. A nichrome film 150 Å thick is deposited from a tungsten coil in vacuum prior to the gold evaporation in order to obtain good adherence. The strip is made by photoresist application with exposure through a contact photographic film, and by subsequent etching steps in a

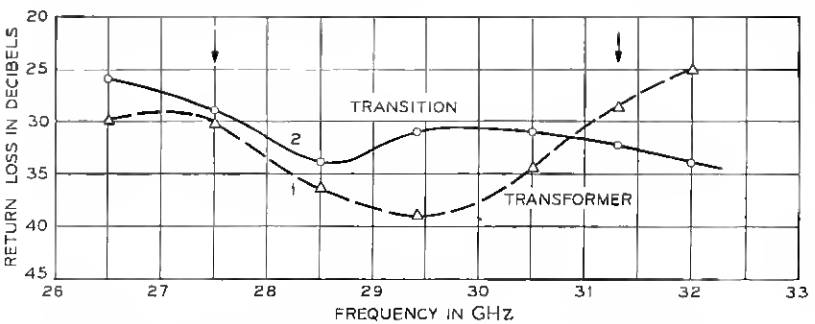

Fig. 4 — Return loss of transformer and transition from waveguide to microstrip from 26.5 GHz to 32 GHz.

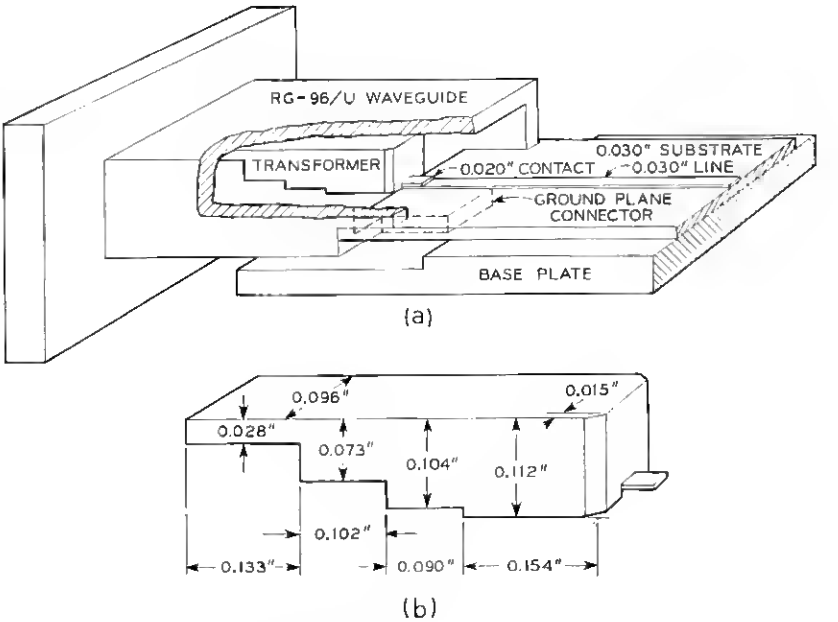

Fig. 5 — Dimensions of waveguide to microstrip transition: (a) mechanical design, (b) ridgeline transformer.

potassium iodine solution for the gold and ferric chloride for the nichrome. The impedance calculated from equations (1), (5), and (7) with $\epsilon_r = 3.78$ is $Z = 75.5$ ohm. Table II gives the results of an attenuation measurement performed with two waveguide-to-microstrip transitions for a 3-inch long microstrip line.

IV. MICROSTRIP IMPATT OSCILLATORS

4.1 *Hybrid Integrated* IMPATT *Circuits*

IMPATT oscillators and bulk sources are required for frequency conversion in repeaters or terminals of solid-state RF systems. Major efforts in the past have been directed towards building sources with high efficiency in waveguide and coaxial circuits. These circuits give satisfactory performance, but present some problems in phase locked applications at higher frequencies or in circuits requiring solid-state devices for power amplifiers of angle-modulated signals. The widest possible locking bandwidth in such a circuit is obtained if the device

is connected to a short at the sbortest possible distance from the diode required for achieving resonance with the effective device reactance. This can be achieved with a microstrip circuit in which one diode terminal is bonded to the ground plane and the other terminal is connected to the strip conductor which is shorted a small distance from the diode. Such a circuit resonates with a minimum of stored electromagnetic energy. It therefore has a low Q and the maximum locking bandwidth for a given injected power.

4.2 *Microstrip Circuit*

Figure 6a shows the microstrip circuit built to obtain the maximum locking range with a given diode. The dimensions of a circuit built at X-band are given in Fig. 6b. The IMPATT oscillator at X-band consists of a silicon avalanche diode in a V package which is mounted in

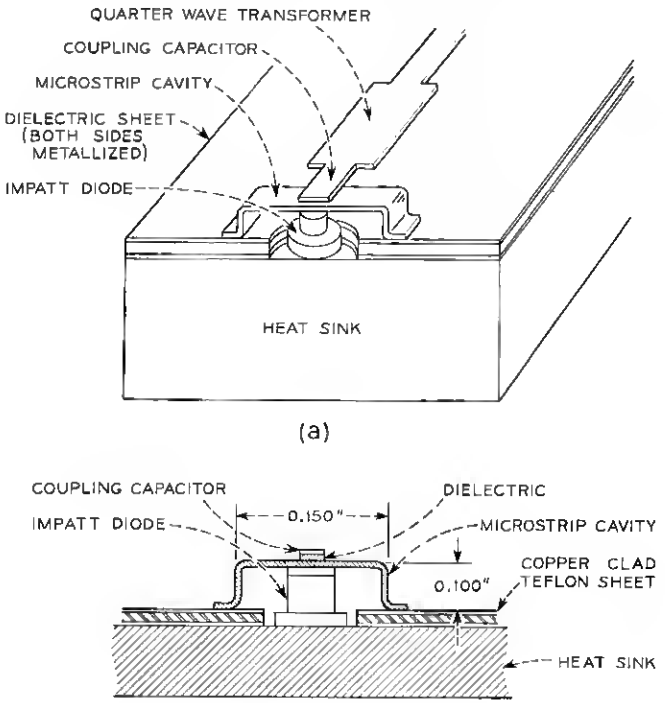

Fig. 6 — Microstrip mount for X-band oscillator: (a) IMPATT oscillator (b) microstrip mount for X-band oscillator.

a short microstrip cavity. A similar circuit built at 30 GHz uses the same passive elements with all physical dimensions smaller. The circuit built at 30 GHz uses an unpackaged diode which is thermocompression-bonded to the heat sink. A loop or small cavity is obtained by mounting the diode in the center of a short microstrip line. The loop acts to a first approximation as a lumped inductance in parallel with the diode. It is observed that the frequency of oscillation multiplied by the square root of the loop length is constant, which means that the oscillation frequency can be changed by varying a single external circuit parameter. This important fact facilitates the circuit design.

Circuits with devices that have a negative impedance characteristic over part of the frequency spectrum present special problems in applying the dc bias. A simple solution has been found for applying the dc bias to devices mounted in microstrip circuits. A thin dielectric sheet with a hole for the diode is mounted on a solid metal block which is also the heat sink for the diode. The dielectric sheet is metallized on both sides and provides an RF bypass with two terminals for applying the dc bias.

The RF coupling between the circuit and the output is obtained with a quarter wavelength microstrip line in series with a coupling capacitor C as shown in Fig. 6. This solution gives dc isolation between circuit and load. The capacitance and the strip line impedance are adjusted for maximum output power. A transition from microstrip to coaxial transmission line is used for measuring the output power at X-band and a transition to waveguide is used for power measurements at 30 GHz.

4.3 *RF Measurements and Locking Experiments*

The circuit parameters and the RF performance obtained with an X-band and a V-band microstrip oscillator are given in Table IV. Locking measurements performed with a V-band oscillator operating at 31.6 GHz and 33.03 GHz are shown in Fig. 7. The diode used in this oscillator has a breakdown voltage of 17 V and a breakdown capacitance of 0.24 pF. The Q of the circuit is defined by

$$\frac{\Delta f}{f_o} = \frac{2}{Q}\left(\frac{P_i}{P_o}\right)^{\frac{1}{2}} \tag{22}$$

where Δf is the locking bandwidth, f_o the frequency of the free-running oscillator, P_o the output power without locking and P_i the in-

TABLE IV—MICROSTRIP IMPATT OSCILLATOR PERFORMANCE

Circuit and diode parameters, RF output	X-band oscillator	V-band oscillator
Microstrip cavity (inches) length, width, height	0.150 0.120 0.100	0.070 0.070 0.020
Silicon IMPATT diode mount	V-type pill package	Epoxy coated for mechanical support
Junction capacitance at breakdown (pF)	0.44	0.22
Breakdown voltage (V)	80	24
Inductance across diode (nH)	0.32	0.16
Coupling capacitance (pF)	0.1	0.01
Oscillator frequency (GHz)	9.6	28.5
RF output (mW)	225	135
Efficiency (%)	2.3	2.2

jected locking power. The value of Q is optimized by adjusting the impedance of the quarter wave transformer and the coupling capacitance. A circuit Q between 3.5 and 5.0 is obtained for a gain from 17 to 30 dB.

4.4 *Hybrid Integration With Other RF Circuits*

The IMPATT oscillator described in this section is built with an external air line microstrip circuit. Hybrid integration of microwave oscillators with other circuits in a solid-state radio system requires a common substrate such as quartz or alumina on which all conductors are simultaneously deposited and then photoetched by photoresist and mask delineation processes. A circuit built with a common substrate consisting of a standard microstrip transmission line requires a hole in the dielectric for the diode. This type of mount is difficult and expensive to make. A better solution is to use the inverted microstrip of Fig. 1c or the triplate microstrip of Fig. 1d with a shunt-mounted diode which is bonded to the ground plane to obtain a good heat sink. The RF bypass shown in Fig. 8 is deposited on the ground plane and two metal studs are bonded to the metallized part of the RF bypass. Additional hybrid circuits may be deposited on the same microstrip line in order to provide other functions, such as downconversion, upconversion, or phase locked operation of oscillators.

V. MICROSTRIP HIGH ORDER VARACTOR MULTIPLIERS

5.1 *Hybrid Integrated Multiplier Circuits*

Frequency multipliers in repeaters and terminals of solid-state radio systems are necessary for driving upconverters and downcon-

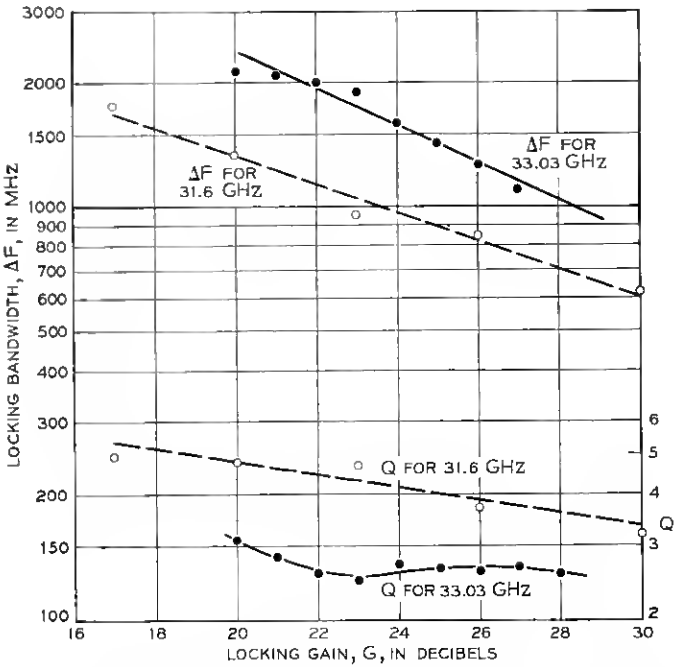

Fig. 7.—Locking range of V-band microstrip oscillator. The oscillation frequency is 31.6 GHz for $I_o = 90$ mA and 33.03 GHz for $I_o = 118$ mA.

verters or for phase-locking solid-state sources such as IMPATT and LSA oscillators. Major efforts in the past have been directed towards building doublers, triplers, and quadruplers with optimized efficiency at specified power levels in waveguide or coaxial circuits. Recently, work has been reported on hybrid integrated multipliers. A quadrupler from 2.25 to 9.0 GHz with two series-mounted silicon diodes on an alumina substrate has given a 4 dB conversion loss with an output power of 800 mW.[11] A hybrid integrated quadrupler from 15 to 60 GHz has been built with gallium arsenide Schottky barrier diodes;[12] a conversion loss of 18 dB has been measured. Quadruplers in the same frequency range have also been built with waveguide circuits. A gallium arsenide Schottky barrier quadrupler from 12.6 to 50.4 GHz, built in a waveguide circuit, has given a conversion loss of 17 to 18 dB. Notice, however, that the same waveguide quadrupler built with diffused junction gallium arsenide diodes has given a highly improved conversion loss of approximately 10 dB because of the beneficial effects of minority carrier charge-storage in the diffused junction.[13]

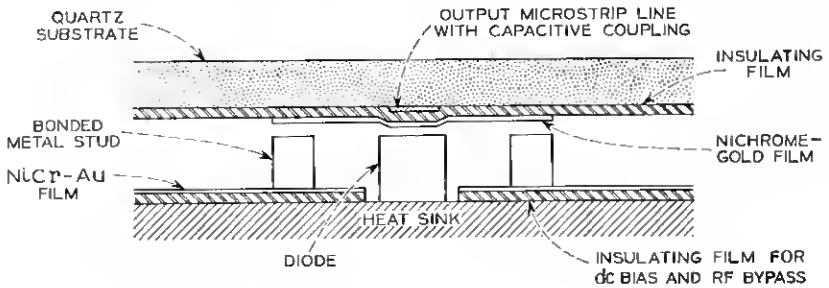

Fig. 8 — IMPATT oscillator cavity with output on inverted microstrip line.

Harmonic generators of order 4 or higher are used in RF systems where high order frequency multiplication from a crystal controlled power source from a few hundred MHz to 10 GHz and above is required. An example is the multiplier used in the short hop radio system which uses a chain consisting of only two stages, an octupler followed by a quadrupler. Lumped elements and waveguide components are used in the chain for all passive circuit elements. It is possible, with present integrated circuit technology, to build the passive elements for the idler circuit and input and output filters on one single insulating substrate. Results obtained with a hybrid integrated octupler from 3.8 to 30.4 GHz are reported in sections 5.2 and 5.3. Results are also given for multipler circuits built on an oversize substrate with an input frequency of 100 MHz and an output frequency of 800 MHz. By linear scaling, whicb means reducing all physical dimensions by the same factor, and by proper scaling of the diode package and the diode characteristics, one can obtain designs for all hybrid integrated octuplers by specifying the input or output frequency of the multiplier. This approach is also useful for designing other components and circuits of an RF repeater such as impedance transformers, directional couplers, filters, upconverters, and downconverters.

5.2 *Microstrip Conductor Configuration for Idlers and Filters*

Idler resonators, and low-pass, and bigh-pass filters for high order multipliers can be built on insulating suhstrates witb transmission line elements shown in Fig. 1. Open-ended or shorted strip conductor stubs are used for tbe idlers, alternating sections of bigb impedance and low impedance microstrip lines for the low-pass filters, and parallel-coupled strip-line resonators for the band-pass filter. The design of these filters has been treated by Matthaei and otbers.[14] Figure 9 shows two micro-

strip conductor configurations which can be used for building a hybrid integrated octupler. It shows a top view of the microstrip conductor pattern which is deposited on an insulating substrate such as quartz or alumina. The varactor diode is shunt-mounted at point D between the strip conductor and the ground plane for obtaining a good heat sink. Quarter wave stubs are used in Fig. 9a for providing the idlers at the second and fourth harmonic of the pump frequency ω_p.

The shortest stub of the F structure is $\lambda/4$ long at the eighth harmonic and is transformed into a short at point A and an open circuit across the diode at D. This prevents power at tbe frequency $8\omega_p$ from flowing back into the pump circuit. The second stub, $\lambda/4$ long at the frequency $4\omega_p$, is transformed into a short at the fourth harmonic at point B and into an open circuit across A. This prevents fourtb harmonic power

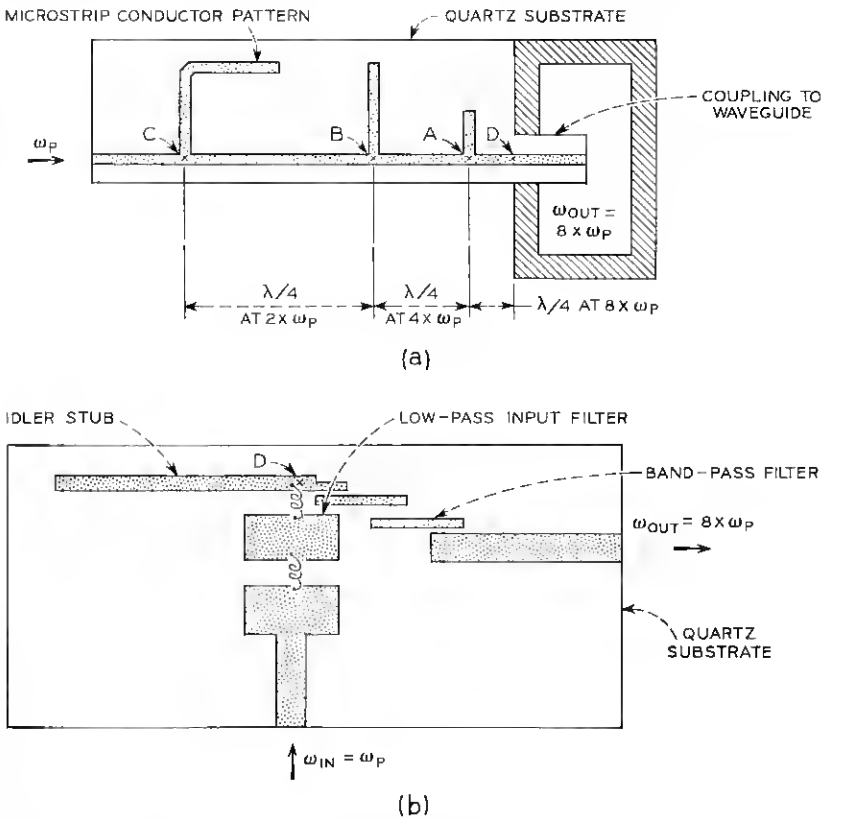

Fig. 9 — Microstrip conductor configuration for high order varactor multipliers: (a) with waveguide output (b) with band-pass filter and microstrip output.

from flowing back into tbe pump circuit. The sbortest stub of the F, tbe section of tbe microstrip between A and D, and tbe sbunt reactance of tbe output circuit, provide tbe idler circuit at the fourtb harmonic. The remaining stub at C, $\lambda/4$ long at $2\omega_p$, has a similar function at tbe second harmonic.

Tbe conductor pattern shown in Fig. 9b is made with a single stub resonator and a sbunt-mounted diode at D. The stub length is designed so that idler currents are flowing at the second barmonic and at least one other higher order barmonic. Microminiature coils are thermocompression bonded between two low impedance microstrip sections for obtaining a two-section low-pass input filter. The two-section parallel-coupled bandpass filter has its center frequency at the eighth harmonic and is designed to reject at least 25 dB at the seventh and ninth harmonic. A transition from microstrip to waveguide for the circuits of Figs. 9a and b is used for measuring the RF performance of the octupler.

5.3 *RF Performance of High Order Multipliers*

The RF output obtained with a higb order multiplier built with the microstrip conductor pattern sbown in Fig. 9a is given in Table V. A coaxial-to-microstrip transition is used at the input of 3.8 GHz and a microstrip-to-RG-96/U waveguide transition is used for measuring the output power. The varactor is a planar diffused gallium arsenide diode which is shunt-mounted at point D between the conductor pattern and the ground plane. This is achieved by using the standard microstrip of Fig. 1a with an additional upper ground plane which is spaced at a distance h from the insulating substrate. Tuning screws are located above points A, B, and C in the upper ground plane in order to maximize the idler currents. The diode terminals are connected between the microstrip pattern and the upper ground plane.

TABLE V—HYBRID INTEGRATED HIGH ORDER MULTIPLIER FROM 3.8 TO 30.4 GHz

Varactor diode	Planar diffused epitaxial GaAs diode
Junction diameter	22 μm
Zero bias capacitance	0.21 pF
Breakdown voltage	18.5 V
Input power at 3.8 GHz coaxial transmission line	200 mW
Output power measured in RG-96/U waveguide	9.6 mW
Conversion loss	13.2 dB

This solution facilitates the assembly and avoids fabrication of a hole in the substrate which is normally done for shunt-mounting solid-state devices. The conductor pattern is deposited on a clear fused quartz subtrate with a thickness of 0.5 mm.

The waveguide provides sufficient rejection for all low order harmonics. The rejection at the seventh and ninth harmonic is lower and a band-pass filter in microstrip would be required in this circuit to suppress the unwanted high order harmonics.

A band-pass filter witb a rejection of 28 dB at tbe seventb barmonic and a 31 dB rejection at tbe ninth barmonic has been built in an oversize microstrip transmission line and in a reduced microstrip line at 30 GHz. Tbe measured 3 dB bandwidtb for the oversize and for tbe reduced filter is ±2.4 percent. Tbe filter consists of two parallel-coupled balf-wavelength resonant microstrip lines on a standard quartz microstrip line. The insertion loss of the oversize model is 0.3 dB at 800 MHz; the measured insertion loss of tbe filter after linear reduction by a factor of 37.5 is 1.8 dB at 30 GHz. From this measurement one concludes that conductor losses are predominant because the insertion loss increases as the square root of the frequency because of the skin effect in the conductor material.

The RF performance of a completely shielded oversize high order multiplier from 100 to 800 MHz with this band-pass filter and with the conductor configuration of Fig. 9b is given in Table VI.

Linear scaling of the measured power levels to higher frequencies is not applicable because no attempt has been made to scale the RC-product of the varactor diode. The main purpose of the experiment is to obtain optimum conductor dimensions in order to build efficient integrated multipliers at much higher frequencies.

VI. CONCLUSION

Hybrid integrated microwave and millimeter wave circuits and components can be built on planar insulating quartz substrates. We

TABLE VI—HIGH ORDER OVERSIZE MULTIPLIER FROM 100 TO 800 MHz

Varactor diode	Planar diffused epitaxial Si diode
Zero bias capacitance	11.5 pF
Breakdown voltage	80 volts
Input power at 100 MHz	975 mW
Output power at 800 MHz	600 mW
Conversion loss	2.1 dB

report the results on the attenuation of microstrip line elements, on transitions from waveguide to microstrip, on IMPATT oscillators, and on high order frequency multipliers. Linear scaling is used for obtaining optimum conductor configurations and for making essential measurements on passive microstrip components. A similar approach can be used for development of other hybrid integrated circuits required for RF systems at 10 GHz and above.

VII. ACKNOWLEDGMENT

The authors express thanks to S. Michael and W. W. Snell for performing exact measurements and to S. Shah for high quality films. IMPATT diodes from B. C. DeLoach and D. F. Ciccolella are gratefully acknowledged.

REFERENCES

1. Ruthroff, C. L., Oshorne, T. L., and Bodtmann, W. F., "Short Hop Radio System Experiment," B.S.T.J., this issue, pp. 1577–1604.
2. Tillotson, L. C., "A Model of a Domestic Satellite Communication System," B.S.T.J., *47*, No. 10 (Decemher 1968), pp. 2111–2137.
3. Engelhrecht, R. S., and Kurokawa, K., "A Wideband Low Noise L-Band Balanced Transistor Amplifier," Proc. IEEE, *53*, No. 3 (March 1965), pp. 237–247.
4. Brenner, H. E., "Computer Design of Suspended-Substrate Integrated Circuits," Microwaves, 7, No. 9 (September 1968), pp. 38–45.
5. Tölke, F., *Praktische Funktionenlehre, Zweiter Band, Theta-Funktionen und speziellе Weierstrass'sche Funktionen,* Berlin: Springer-Verlag, 1966, pp. 1–83.
6. Wheeler, H. A., "Transmission-Line Properties of Parallel Strips Separated by a Dielectric Sheet," IEEE Trans. Microwave Theory and Techniques, *MTT-13*, No. 2 (March 1965), pp. 172–185.
7. Grieg, D. D. and Engelmann, H. F., "Microstrip—A New Transmission Technique for the Kilomegacycle Range," Proc. IRE, *40*, No. 12 (Decemher 1952), pp. 1644–1650.
8. Arditi, M., "Characteristics and Applications of Microstrip for Microwave Wiring," IEEE Trans. on Microwave Theory and Techniques, *MTT-3*, No. 2 (March 1955), pp. 31–56.
9. Cohn, S. B., "Optimum Design of Stepped Transmission-Line Transformers," IRE Trans. on Microwave Theory and Techniques, *MTT-3*, No. 3 (April 1955), pp. 16–21.
10. Hopfer, S., "The Design of Ridged Waveguides," IRE Trans. on Microwave Theory and Techniques, *MTT-3*, No. 5 (Octoher 1955), pp. 20–29.
11. Johnson, K. M., "A High-Performance Integrated Microwave Circuit Frequency Quadrupler," IEEE Trans. on Microwave Theory and Techniques, *MTT-16*, No. 7 (July 1968), pp. 420–424.
12. Mao, S., Jones, S., and Vendelin, G. D., "Millimeter-Wave Integrated Circuits," IEEE Trans. on Microwave Theory and Techniques, *MTT-16*, No. 7 (July 1968), pp. 455–461.
13. Lee, T. P., and Burrus, C. A., "A Millimeter-Wave Quadrupler and an Up-Converter Using Planar-Diffused Gallium Arsenide Varactor Diodes," IEEE Trans. on Microwave Theory and Techniques, *MTT-16*, No. 5 (May 1968), pp. 287–296.
14. Matthaei, G. L., Young, L., and Jones, E. M. T., *Microwave Filters, Impedance Matching Networks, and Coupling Structures,* New York: McGraw-Hill, 1964, pp. 355–477.